

Demystifying Self-supervised Trojan Attacks

Changjiang Li[†] Ren Pang[†] Zhaohan Xi[†] Tianyu Du[†]

Shouling Ji[‡] Yuan Yao[§] Ting Wang[†]

[†]Pennsylvania State University [‡]Zhejiang University [§]Nanjing University

Abstract—As an emerging machine learning paradigm, self-supervised learning (SSL) is able to learn high-quality representations for complex data without data labels. Prior work shows that, besides obviating the reliance on labeling, SSL also benefits adversarial robustness by making it more challenging for the adversary to manipulate model prediction. However, whether this robustness benefit generalizes to other types of attacks remains an open question.

We explore this question in the context of trojan attacks by showing that SSL is comparably vulnerable as supervised learning to trojan attacks. Specifically, we design and evaluate CTRL, an extremely simple self-supervised trojan attack. By polluting a tiny fraction of training data ($\leq 1\%$) with indistinguishable poisoning samples, CTRL causes *any* trigger-embedded input to be misclassified to the adversary’s desired class with a high probability ($\geq 99\%$) at inference. More importantly, through the lens of CTRL, we study the mechanisms underlying self-supervised trojan attacks. With both empirical and analytical evidence, we reveal that the representation invariance property of SSL, which benefits adversarial robustness, may also be the very reason making SSL highly vulnerable to trojan attacks. We further discuss the fundamental challenges to defending against self-supervised trojan attacks, pointing to promising directions for future research.

1. Introduction

As a new machine learning paradigm, self-supervised learning (SSL) has gained tremendous advances recently [4], [11], [6]. Without requiring data labeling or human annotations, SSL is able to learn high-quality representations for complex data and enable a range of downstream tasks. In particular, contrastive learning, one dominant SSL approach [4], [11], [6], [5], [13], performs representation learning by aligning the features¹ of the same sample under varying data augmentations (*e.g.*, random cropping) while separating the features of different samples. In many tasks, contrastive learning has attained performance comparable to supervised learning [11]. Meanwhile, besides obviating the reliance on data labeling, SSL also benefits the robustness to adversarial examples, label corruption, and common input corruptions by making it more challenging for the adversary to influence model prediction directly [17]. However, whether

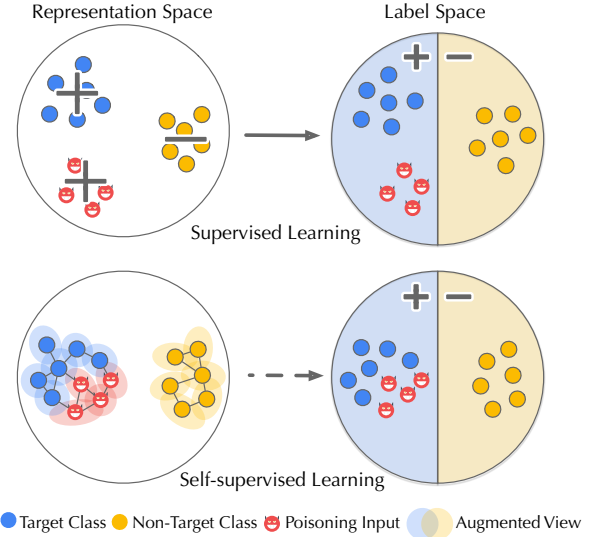


Figure 1: Comparison of supervised and self-supervised trojan attacks (note: self-supervised trojan attacks influence the label space only indirectly through the representations).

this robustness benefit generalizes to other malicious attacks remains an open question.

In this work, we explore this question in the context of trojan attacks. Supervised trojan attacks [50], [54], [35] that plant malicious functions (“backdoors”) into models by poisoning training data with corrupted inputs *and* labels, are inapplicable to SSL due to label absence. While recent work has explored new ways of injecting backdoors into SSL-trained models [39], [30], [2], [22], the existing attacks seem to significantly under-perform their supervised counterparts: they either work for specific, pre-defined inputs only [22], [30] or succeed with a low probability (*e.g.*, $\leq 2\%$ on ImageNet-100) [39]. These observations raise a set of intriguing and critical questions:

- RQ₁ – *Is SSL inherently more resilient to trojan attacks?*
- RQ₂ – *If not, what makes SSL equally vulnerable?*
- RQ₃ – *What are the potential countermeasures and challenges to mitigate such vulnerability?*

Our work – This work represents a solid initial step towards answering these questions.

RA₁ – We present CTRL,² a simple yet effective trojan

1. Below we use the terms “feature” and “representation” exchangeably.

2. CTRL: Contrastive Trojan Learning.

attack against contrastive learning. Compared with the existing attacks, (i) CTRL assumes that the adversary is able to pollute a tiny fraction of training data but without any control of the training process; (ii) it defines the trigger as a specific perturbation in the spectral space of inputs and generates poisoning data highly indistinguishable from clean data; and (iii) it aims to force *all* trigger-embedded inputs to be misclassified to the adversary’s desired class at inference. We demonstrate the effectiveness of CTRL through extensive evaluation using benchmark contrastive learning methods, models, and datasets. For instance, by poisoning $\leq 1\%$ of the training data, CTRL attains $\geq 99\%$ attack success rate on CIFAR-10, comparable to supervised trojan attacks.

RA₂ – Moreover, through the lens of CTRL, we reveal the unique vulnerability incurred by the current design of SSL methods. Intuitively, CTRL exploits data augmentation and contrastive loss, two key ingredients of SSL, that together entail “representation invariance” – different augmented views of the same input share similar representations. Given the overlap between the augmented views of trigger-embedded and target-class inputs, enforcing representation invariance naturally entangles them in the feature space, as illustrated in Figure 1, leading to the risk of trojan attacks. This mechanism fundamentally differs from supervised trojan attacks, which directly associate the trigger pattern with the target class in the label space, while the representations of trigger-embedded and target-class inputs are not necessarily aligned [44].

RA₃ – Finally, we discuss potential countermeasures to mitigate CTRL and explore the challenges to defending against self-supervised trojan attacks in general. We consider design options including re-defining contrastive loss, ablating augmentation operators, performing data sanitization before pre-training, and applying run-time detection. For instance, SCAN [44], a state-of-the-art defense against supervised trojan attacks, detects trigger-embedded inputs based on the statistical properties of their representations. However, we find SCAN ineffective against CTRL, due to the inherent entanglement between the representations of trigger-embedded and target-class inputs. We conclude that defending against self-supervised trojan attacks entails unique challenges, pointing to several research directions.

Our contributions – To our knowledge, this work represents the first systematic study on the vulnerability of the contrastive learning paradigm (SSL in general) to trojan attacks. Our contributions are summarized as follows.

- We present CTRL, a simple yet effective self-supervised trojan attack. Leveraging CTRL, we show that SSL is comparably vulnerable as supervised learning to trojan attacks. Our findings imply that the benefit of SSL for adversarial robustness may not generalize to trojan attacks.

- With both empirical and analytical evidence, we show that supervised and self-supervised trojan attacks function through fundamentally different mechanisms, the former by associating trigger patterns with target-class labels, while the latter by entangling the representations of trigger-embedded inputs and target-class inputs. We further reveal that the representation invariance property of SSL, which benefits

adversarial robustness, may also account for the vulnerability of SSL to trojan attacks.

- We explore a variety of potential mitigation against the threats of trojan attacks under the SSL setting and characterize their unique challenges, which point to several promising directions for further research.

Roadmap – The remainder of this paper is structured as follows. § 2 introduces the fundamental concepts and assumptions; § 3 presents the high-level design of CTRL and its implementation; § 4 empirically evaluates CTRL and compares it with the state-of-the-art attacks; § 5 studies the mechanisms underlying supervised and self-supervised trojan attacks, and discusses potential defenses against CTRL; § 6 surveys relevant literature; the paper is concluded in § 7.

2. Preliminaries

We first introduce fundamental concepts and assumptions used throughout the paper.

2.1. Self-supervised Learning

Deep neural networks (DNNs) represent a class of machine learning models to learn high-level abstractions for complex data. In a predictive task, a DNN h_θ (parameterized by θ) encodes a function $h_\theta : \mathbb{R}^n \rightarrow \mathbb{S}^m$, where n and m denote the input dimensionality and the number of classes. A DNN typically comprises two parts $h = g \circ f$ wherein f is the encoder that extracts features (*i.e.*, latent representations) from given inputs while g is the classifier that maps such representations to output classes. Under the supervised setting, to train a DNN h , the training algorithm uses a training set \mathcal{D} , in which each instance (x, y) comprises input x and its ground-truth label y , and optimizes h ’s parameters θ with respect to a loss function $\mathbb{E}_{(x,y) \in \mathcal{D}} \ell(h_\theta(x), y)$ (*e.g.*, the cross entropy of $h_\theta(x)$ and y).

However, supervised learning is inapplicable when data labeling is scarce or expensive (*e.g.*, massive data crawled from the Web). Recently, self-supervised learning (SSL) is emerging as a new paradigm for such settings. Using the supervisory signals from the data itself, SSL trains a high-quality encoder f , which can then be integrated with a downstream classifier g and fine-tuned with weak supervision to form the end-to-end model.

Conceptually, SSL can be categorized as generative and contrastive [20]. In this paper, we mainly focus on contrastive learning that performs representation learning by optimizing *alignment* – aligning the latent representations of the same sample under varying data augmentations (*i.e.*, “positive pairs”), and/or *uniformity* – separating the representations of the augmented views of different samples (*i.e.*, “negative pairs”). Below, we introduce three representative contrastive learning methods, as illustrated in Figure 2.

SimCLR [4] maximizes the similarity of positive pairs relative to the similarity of negative pairs. Specifically, at each iteration, it performs randomly selected augmentations over each input to generate its “augmented views”. For each input

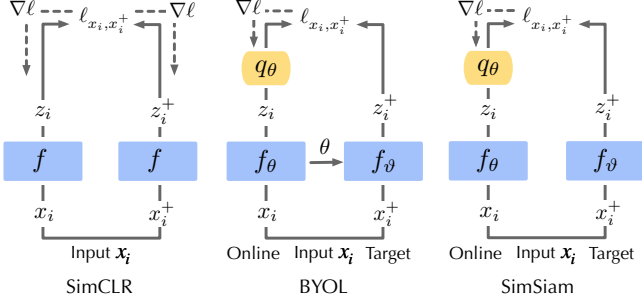


Figure 2: Illustration of representative contrastive learning methods.

x_i , a pair of its augmented views (x_i, x_i^+) forms a positive pair, while a set of augmented views of other inputs \mathcal{N}_{x_i} form its negative pairs. Let z_i denote the latent representation of view x_i (i.e., $z_i = f(x_i)$).³ The contrastive loss of the pair (x_i, x_i^+) is defined by the InfoNCE loss [48]:

$$\ell_{x_i, x_i^+} = -\log \frac{\exp(\frac{\text{sim}(z_i, z_i^+)}{\tau})}{\sum_{x_j^- \in \mathcal{N}_{x_i}} \exp(\frac{\text{sim}(z_i, z_j^-)}{\tau}) + \exp(\frac{\text{sim}(z_i, z_i^+)}{\tau})} \quad (1)$$

where $\text{sim}(\cdot, \cdot)$ is the similarity function (e.g., cosine similarity) and τ denotes the temperature parameter.

BYOL [11] employs two asymmetric networks, the online and target networks, where the target network provides the regression target to train the online network, as illustrated in Figure 2. Specifically, the online network (parameterized by θ) consists of an encoder f_θ and a predictor q_θ , while the target network (parameterized by ϑ) comprises only the encoder f_ϑ . Similar to SimCLR, BYOL generates a pair of augmented views (x_i, x_i^+) for each input and defines the contrastive loss as:

$$\ell_{x_i, x_i^+} = \|q_\theta(f_\theta(x_i)) - f_\vartheta(x_i^+)\|_2^2 \quad (2)$$

where both $q_\theta(f_\theta(x_i))$ and $f_\vartheta(x_i^+)$ are L_2 normalized and the overall loss is symmetrized by computing over both (x_i, x_i^+) and (x_i^+, x_i) . The online network is optimized with respect to Eq (2), where the stop gradient operator is applied on f_ϑ ; meanwhile, the target network is updated using an exponential moving average operator: $\vartheta = \eta\vartheta + (1 - \eta)\theta$, where η is the moving average hyper-parameter.

SimSiam [6] is a variant of BYOL, which differs mainly in removing the exponential moving average operator, as illustrated in Figure 2.

2.2. Trojan Attacks

Trojan attacks represent one major threat to the security of DNNs [12], [33], [35], [28]. As illustrated in Figure 3, the adversary plants “backdoors” into the victim’s model during training and activates such backdoors with “triggers” at inference. Typically, the infected model (trojan model) reacts to trigger-embedded inputs (trigger inputs) in a highly

3. Strictly speaking, the *projector*, a small multi-layer perception network, is often applied on $f(x_i)$ to produce z_i , which is omitted for simplicity.

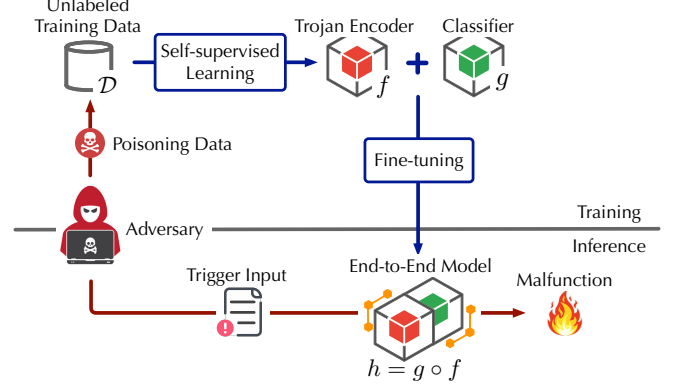


Figure 3: Illustration of trojan attacks in contrastive learning.

predictable manner (e.g., classified to the adversary’s desired class) but functions normally otherwise. Formally, under the supervised setting, the loss function of trojan attacks via poisoning training data is defined as:

$$\mathbb{E}_{(x,y) \in \mathcal{D}} \ell(h(x), y) + \lambda \mathbb{E}_{x_* \in \mathcal{D}_*} \ell(h(x_*), t) \quad (3)$$

where ℓ denotes the prediction loss, \mathcal{D} and \mathcal{D}_* are the clean and poisoning training data respectively, t is the target class desired by the adversary, and the parameter λ balances the influence of \mathcal{D} and \mathcal{D}_* (e.g., by controlling their ratio).

Trojan attacks are of particular interest for SSL: as SSL-trained models are subsequently used in various downstream tasks, trojan attacks may cause widespread damage. Yet, most supervised trojan attacks are inapplicable to self-supervised learning due to label absence. Recent work has explored new ways of injecting backdoors into SSL-trained models. Below, we introduce three representative attacks.

SSLBackdoor [39] defines a specific image patch as the trigger and generates poisoning data by attaching the patch to inputs from the target class. With random cropping, the trigger is retained in certain augmented views and removed in the others. Therefore, by aligning the positive pairs of trigger inputs, the representation of the trigger pattern is associated with the target-class inputs. However, due to its reliance on (i) whether random cropping is selected as the augmentation and (ii) whether the trigger is preserved, the attack suffers a low attack success rate (e.g., $\leq 2\%$ on ImageNet-100).

BadEncoder [22] defines an objective function that associates trigger patterns with reference inputs from the target class in the representation space so that any trigger inputs are misclassified into the target class in the downstream tasks. However, compared with other self-supervised trojan attacks, BadEncoder assumes a stronger threat model in which the adversary has control over the training process.

PoisonedEncoder [30] targets a specific set of inputs and creates poisoning data by combining such inputs with their reference inputs in the representation space. Compared with other self-supervised trojan attacks, PoisonedEncoder is limited in that it only works on a set of pre-defined inputs rather than any trigger-embedded inputs.

Overall, the existing self-supervised trojan attacks seem to under-perform their supervised counterparts, raising the

intriguing question: is SSL inherently more resilient than supervised learning to trojan attacks?

3. CTRL: A Simple yet Effective Trojan Attack

To answer the above question, we present CTRL, an extremely simple self-supervised trojan attack with performance comparable to its supervised counterparts.

3.1. Threat Model

Following the existing work on trojan attacks [12], [33], [35], we assume the threat model below.

Attacker’s objective – The adversary aims to inject malicious functions into the target model during training, such that at inference, any input embedded with a predefined trigger is classified into the adversary’s target class while the model functions normally on clean inputs.

Attacker’s capability – The adversary attains the objective by polluting a tiny fraction of the victim’s training data. Note that this assumption is practical for SSL as it often uses massive unlabeled data collected from public data sources (e.g., Web), which opens the door for the adversary to pollute such sources and lure the victim to download and use poisoning data during training.

Attacker’s knowledge – We assume a black-box setting in which the adversary has no knowledge about (i) the encoder and classifier models or (ii) the training and fine-tuning methods (e.g., classifier-only versus full-model tuning).

3.2. Attack Overview

In a nutshell, CTRL comprises three functions as sketched in Algorithm 1: *DefineTrigger* – designing an augmentation-agnostic trigger pattern; *SelectCandidate* – selecting a set of candidate inputs from a reference dataset; and *ApplyTrigger* – applying the trigger to each candidate input to generate the poisoning data.

Algorithm 1: CTRL Attack

Input: t : target class; k : number of poisoning inputs; $\tilde{\mathcal{D}}$: reference dataset; δ : perturbation magnitude

Output: \mathcal{D}_* : poisoning dataset

```

1  $r \leftarrow \text{DefineTrigger}(\delta)$ ;
2  $\mathcal{D}_* \leftarrow \text{SelectCandidate}(\tilde{\mathcal{D}}, t, k)$ ;
3 foreach  $x_* \in \mathcal{D}_*$  do update  $x_* \leftarrow \text{ApplyTrigger}(x_*, r)$ ;
4 release  $\mathcal{D}_*$ ;

```

Compared with the existing self-supervised trojan attacks, CTRL differs in its fundamental design of leveraging SSL to inject backdoors. Specifically, as illustrated in Figure 4, existing attacks rely on *asymmetric* augmented views: within each positive pair of a trigger input, one view must contain the trigger and the other must not, such that aligning this pair associates the trigger pattern with the target-class input [39]. While intuitive, this design hinges on the occurrence of specific trigger-augmentation interaction (e.g., random cropping cuts out an image patch), resulting in low utilization

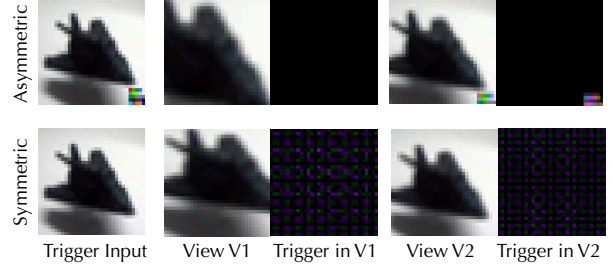


Figure 4: Symmetric and asymmetric augmented views (note: the trigger in the symmetric case is magnified by 20 times to be evident).

of the poisoning data. In comparison, CTRL uses *symmetric* augmented views: it ensures that the trigger is preserved in most augmented views of trigger inputs, regardless of the underlying augmentations; aligning such augmented views naturally entangles trigger-embedded and target-class inputs (details in § 5). Due to its less reliance on the augmentations, this design fully utilizes the poisoning data and largely improves the attack effectiveness.

3.3. Implementation

Next, we elaborate on the implementation of CTRL to fulfill the above design.

DefineTrigger – To realize symmetric augmented views, we apply spectral triggers [51], which are defined as specific perturbations to inputs’ frequency domain (e.g., increase the magnitude of a particular frequency band by 50). Spectral triggers possess the following properties: (i) *augmentation-agnostic* – they are global (covering the entire input) and repetitive (periodic in the input’s spatial domain), making them insensitive to augmentations. The triggers are thus retained in the augmented views regardless of the augmentations. (ii) *inspection-evasive* – they are defined as negligible perturbations to the input’s high-frequency bands, leading to invisible patterns such that the poisoning data is indistinguishable from the clean data. (iii) *control-flexible* – they allow the adversary to flexibly control the trigger magnitude in the spectral space to balance different attack metrics. We explore alternative designs in § 4.

SelectCandidate – After defining trigger r , we generate the poisoning data \mathcal{D}_* by applying r to a set of candidate inputs. To this end, we assume the adversary has access to a small set of target-class inputs $\tilde{\mathcal{D}}$. Recall that the adversary has no control over which inputs to be used in training. To maximize the chance of poisoning data being selected, the adversary may use all the inputs in $\tilde{\mathcal{D}}$, while the victim may then randomly select a subset in training. To imitate the process, we randomly sample k inputs from $\tilde{\mathcal{D}}$ to craft \mathcal{D}_* . We also empirically evaluate alternative scenarios in § 4.

ApplyTrigger – To apply the spectral trigger r , we first convert a given input x from the RGB space to the $YCbCr$ space. The conversion separates x ’s luminance component (Y) from its chrominance component (C_b and C_r). As human perception is insensitive to changes in the chrominance [16],

we apply perturbation in the C_b and C_r channels only. In the selected channel, we divide x into disjoint blocks (e.g., 32×32). We apply discrete cosine transform (DCT) [38] on each block to transform it from the spatial domain to the frequency domain. As most of x 's energy is concentrated in the low-frequency bands, we apply the perturbation defined in r (e.g., increasing the magnitude by 50) on selected high-frequency bands, which tends to cause invisible distortion. We then apply inverse DCT to transform the blocks back to the spatial domain and stitch them together.

Finally, we convert the input from YC_bC_r to RGB to form the trigger input. This process is illustrated in Figure 5.

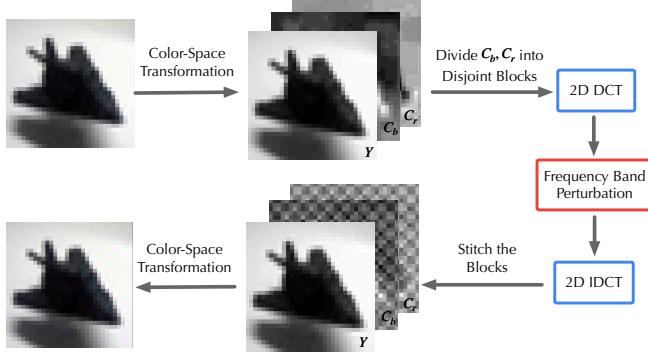


Figure 5: Illustration of the process of trigger generation.

Note that as the spectral trigger is defined as increasing the magnitude of specific frequency bands, it is possible to decouple the setting of triggers for crafting poisoning data (i.e., low magnitude to optimize the attack evasiveness) and activating backdoors at inference time (i.e., high magnitude to optimize the attack effectiveness).

4. Evaluation

Next, we conduct an empirical evaluation of CTRL, which is designed to answer the following questions:

Q₁: Is CTRL effective against popular SSL methods?

Q₂: What factors may influence its effectiveness?

Q₃: How does each component contribute to its effectiveness?

4.1. Experimental Setting

We begin by introducing the main setting of our evaluation. More details are deferred to Appendix B.

Datasets – Our evaluation primarily uses three benchmark datasets for SSL methods: CIFAR-10 [26] consists of 60,000 32×32 color images divided into 10 classes; CIFAR-100 [27] is similar to CIFAR-10 but includes 100 classes, each of 600 images; ImageNet-100 is a subset sampled from the ImageNet-1K dataset [8] and contains 100 randomly selected classes, each of 1,350 images re-scaled to 64×64 . Besides, under the setting that the pre-training and downstream datasets are different, we also use GTSRB, which contains 51,839 32×32 traffic-sign images in 43 classes, as an additional dataset.

SSL methods – We mainly use three representative contrastive learning methods, SimCLR [4], BYOL [11], and SimSiam [6]. Table 1 summarizes their accuracy on the above benchmark datasets.

Dataset	SSL Method					
	SimCLR		BYOL		SimSiam	
	ACC	ASR	ACC	ASR	ACC	ASR
CIFAR-10	79.1%	9.93%	82.4%	12.2%	81.5%	11.75%
CIFAR-100	48.1%	1.14%	51.0%	0.46%	52.0%	0.72%
ImageNet-100	42.2%	1.59%	45.1%	1.41%	41.3%	1.53%

Table 1. Accuracy of different SSL methods under normal training.

Models – By default, we use an encoder with ResNet-18 [14] as its backbone and a two-layer MLP projector to map the representations to a 128-dimensional latent space; further, we use a two-layer MLP with the hidden-layer size of 128 as the downstream classifier. We also explore alternative architectures in § 4.1. Following prior work [4], [6], we consider random resized cropping, random horizontal flipping, color distortions, and random grayscale as the set of augmentation operators.

Attacks – Given the limited prior work on self-supervised trojan attacks, we compare CTRL with two baseline attacks due to their similar threat model: SSLBackdoor [39] defines the trigger pattern as a 5×5 image patch placed at a random position of each input. PoisonedEncoder [30] targets specific inputs and combines target inputs with reference inputs to generate poisoning samples. By default, CTRL defines the trigger pattern as increasing the magnitude of selected high-frequency bands (e.g., 31) of given inputs. By default, we set the magnitude increase as 50 for crafting the poisoning data and 100 for activating backdoors at inference. Figure 6 compares the poisoning samples of different attacks.

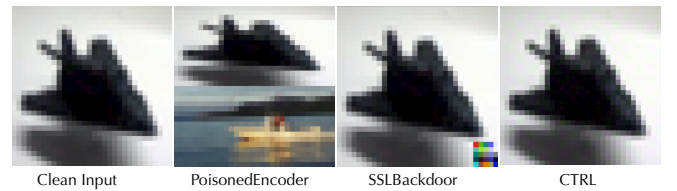


Figure 6: Comparison of the poisoning samples of different attacks.

Metrics – We mainly use two metrics, attack success rate (ASR) and clean data accuracy (ACC). Intuitively, ASR is defined as the trojan model’s accuracy of classifying trigger inputs to the adversary’s target class during inference, which measures the attack effectiveness, while ACC is defined as the trojan model’s accuracy of correctly classifying clean inputs, which measures the attack evasiveness. Further, in the transfer setting where the pre-training and downstream datasets are different, we consider untargeted attacks and measure ASR as the trojan model’s accuracy drop on trigger inputs. We repeat each experiment three times and report the average results.

Attack	Dataset	SSL Method					
		SimCLR		BYOL		SimSiam	
		ACC	ASR	ACC	ASR	ACC	ASR
Poisoned-Encoder	CIFAR-10	80.5%	11.1%	81.7%	10.7%	81.9%	10.7%
	CIFAR-100	47.9%	1.3%	50.9%	1.2%	52.3%	1.2%
	ImageNet-100	41.9%	1.0%	44.8%	1.4%	41.5%	1.3%
SSL-Backdoor	CIFAR-10	80.0%	10.5%	82.3%	11.2%	81.9%	10.7%
	CIFAR-100	48.3%	1.2%	50.4%	1.2%	52.2%	1.2%
	ImageNet-100	42.0%	1.1%	45.4%	1.2%	41.2%	1.3%
CTRL	CIFAR-10	80.5%	85.3%	82.2%	61.9%	82.0%	74.9%
	CIFAR-100	47.6%	68.8%	50.8%	42.3%	52.6%	83.9%
	ImageNet-100	42.2%	20.4%	45.9%	37.9%	40.2%	39.2%

Table 2. Effectiveness of CTRL and baseline attacks.

Q1: Attack Effectiveness

Targeted attacks. We evaluate the effectiveness of different attacks against representative SSL methods on benchmark datasets. For a fair comparison, we fix the poisoning ratio of all the attacks as 1%. The results are summarized in Table 2. We have the following observations.

CTRL – Across different settings of datasets and SSL methods, CTRL attains the highest attack effectiveness. For instance, it achieves 83.9% ASR on CIFAR-100 when the trojan model is trained using SimSiam, much higher than its clean accuracy. Besides, compared with Table 1, CTRL has little impact on the model’s performance on clean input. For instance, the trojan model performs even slightly better than the clean model on CIFAR-10 under SimCLR.

SSLBackdoor – In comparison, SSLBackdoor is ineffective. In most cases, its performance is close to random guess (e.g., around 10% on CIFAR-10). This may be explained by its asymmetric design: it requires to (i) select random cropping as the augmentation and (ii) retain and remove the trigger in two augmented views, respectively. The low probability that the two conditions are met simultaneously results in the poor utilization of poisoning data in SSLBackdoor.

PoisonedEncoder – Meanwhile, the effectiveness of PoisonedEncoder is also limited. Recall that PoisonedEncoder only targets specific inputs by combining the target inputs with reference inputs together during poisoning (cf. Figure 6), thereby unable to generalize to all trigger-embedded inputs. Therefore, the ASR of PoisonedEncoder is bounded by the poisoning ratio (i.e., 1%).

Untargeted attacks. In the transfer scenario, the victim trains an encoder on a pre-training dataset using SSL and then fine-tunes the downstream classifier using another dataset. Next, we measure the attack effectiveness under this setting. Given the pre-training and downstream datasets tend to have different class distributions, we consider untargeted attacks and measure the attack effectiveness by the models’ accuracy drop on trigger inputs. Figure 7 shows the trojan models’ accuracy in classifying clean and trigger inputs when the pre-training dataset is CIFAR-10 or CIFAR-100.

Specifically, even if the pre-training and downstream datasets are different, CTRL greatly decreases the model’s accuracy in classifying trigger inputs. For example, with

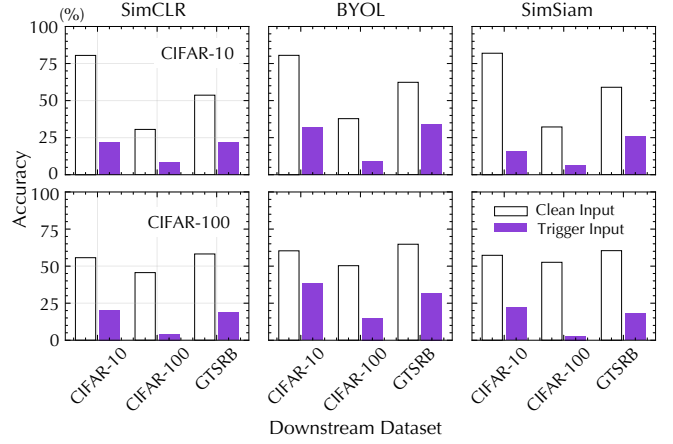


Figure 7: Model accuracy of classifying clean and trigger input under the transfer setting.

CIFAR-100 and CIFAR-10 as the pre-training and downstream datasets, the trojan model trained using SimCLR achieves the accuracy of 55.7% and 20.5% on clean and trigger inputs, respectively. This large gap indicates a highly effective untargeted attack. Further, we find that even if the downstream dataset does not contain the adversary’s target class, the trigger inputs tend to be misclassified to certain classes (in the downstream dataset) that are semantically similar to the target class (in the pre-training dataset). For instance, if the target class is set as “truck” in CIFAR-10 (pre-training), most trigger inputs are classified to the sub-classes of the “vehicle” super-class in CIFAR-100 (downstream) such as “bus”, “pickup truck”, and “train”.

Q2: Influential Factors

Next, we explore a set of key factors that may impact the effectiveness of CTRL.

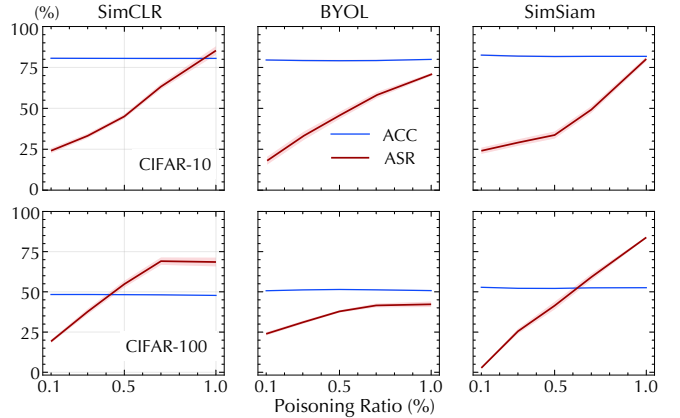


Figure 8: Performance of CTRL w.r.t. the poisoning ratio.

Poisoning ratio. Figure 8 shows how the performance of CTRL varies as the poisoning ratio increases from 0.1% to 1%. We observe that increasing the poisoning ratio has little impact on the trojan model’s performance of classifying clean inputs, but greatly increases the attack effectiveness.

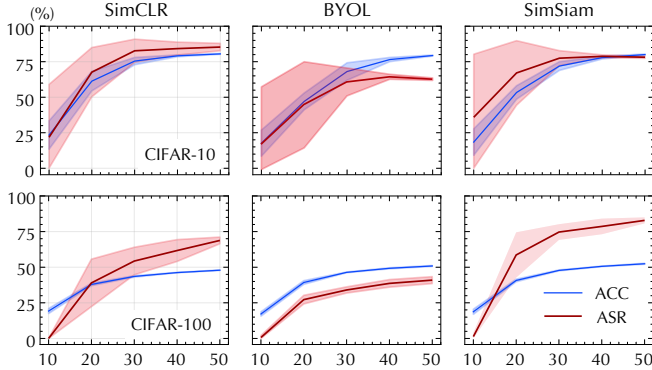


Figure 9: Performance of CTRL w.r.t. the fine-tuning data size.

For example, as the poisoning ratio varies from 0.1% to 1%, the ASR of CTRL increases by 61.2% on CIFAR-10 with SimCLR. Further, even with a 0.5% poisoning ratio (*e.g.*, 100 out of 50,000 training samples), the adversary still injects effective backdoors into the trojan models (*e.g.*, close to 50% ASR on CIFAR-10 with SimCLR), indicating the practicality of CTRL in a real-world setting, in which the adversary is often able to pollute a limited amount of training data.

Fine-tuning data size. Typically, equipped with the pre-trained encoder, the victim fine-tunes the downstream classifier with a small labeled dataset. Here, we evaluate the impact of this fine-tuning dataset on CTRL. Figure 9 illustrates the performance of CTRL as a function of the number of labeled samples per class.

Observe that both ACC and ASR of CTRL increase with the fine-tuning data size, while their variance decreases gradually. For instance, when the number of labeled samples per class is set as 50, the ASR of CTRL on CIFAR-10 under SimSiam stably remains around 75%. This may be explained as follows. Without the supervisory signal of labeling, CTRL achieves effective attacks by entangling the representations of trigger-embedded and target-class inputs (details in § 5). During fine-tuning, more labeled samples imply that the representations of trigger-embedded inputs are more likely to be associated with the target-class label, leading to higher and more stable ASR. In other words, more fine-tuning data not only improves the model’s performance but also increases its attack vulnerability.

Batch size. Existing studies show that batch size tends to impact the performance of contrastive learning [6]. Here, we explore its influence on the performance of CTRL. Specifically, on the CIFAR-10, we measure the ACC and ASR of CTRL with the batch size varying from 128 to 512, with results shown in Figure 10.

Observe that the model’s accuracy improves with the batch size, which corroborates the existing studies [6]. Moreover, a larger batch size (*e.g.*, ≥ 512) generally benefits the ASR of CTRL. This may be explained by that more positive pairs (also more negative pairs in SimCLR) in the same batch lead to tighter entanglement between trigger-embedded and target-class inputs. Meanwhile, for smaller batch sizes (*e.g.*,

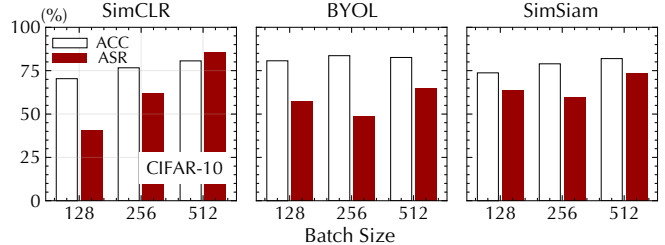


Figure 10: Performance of CTRL w.r.t. the batch size on CIFAR10.

≤ 256), the three SSL methods show slightly different trends. This may be attributed to the design of their loss functions: BOYL and SimSiam only optimize positive pairs, while SimCLR optimizes both positive and negative pairs, thereby gaining more benefits from larger batch sizes.

Encoder model. The previous experiments are conducted on an encoder with ResNet-18 as its backbone. We now evaluate the impact of the encoder model on the performance of CTRL on CIFAR-10. We evaluate the ACC and ASR of CTRL on encoders of various architectures including ShuffleNet-V2 [34], MobileNet-V2 [40], and SqueezeNet [19], with the other settings fixed the same as Table 2.

Encoder Model	ACC	ASR
ResNet-18	80.5%	85.3%
MobileNet-V2	76.4%	79.8%
SqueezeNet	74.7%	54.8%
ShuffleNet-V2	76.2%	38.3%

Table 3. Evaluation on different model architectures.

As shown in Table 3, beyond ResNet-18, CTRL attains high ASR across all the other architectures (*e.g.*, 79.8% ASR on MobileNet-V2), indicating its insensitivity to the encoder model. Further, observe that both ACC and ASR of CTRL are slightly lower on MobileNet, SqueezeNet, and ShuffleNet, compared with ResNet, implying a possible accuracy-robustness trade-off [46]. We consider investigating this trade-off as our ongoing research.

Fine-tuning method. In fine-tuning the downstream classifier, the victim may use different strategies (*e.g.*, classifier-only versus full-model tuning). Recall that the adversary has no knowledge or control over the fine-tuning. Here, we evaluate the impact of the fine-tuning strategy on the attack performance. Table 4 summarizes the ACC and ASR of CTRL on CIFAR-10 under SimCLR with varying fine-tuning strategy and trigger magnitude. We have the following observations.

Trigger Magnitude	Fine-tuning Method	ACC	ASR
50	classifier-only	80.6%	67.3%
	full-model	84.4%	65.1%
100	classifier-only	81.1%	86.3%
	full-model	84.5%	71.7%

Table 4. Performance of CTRL w.r.t. fine-tuning strategy and trigger magnitude on CIFAR-10 under SimCLR.

First, compared with classifier-only tuning, fine-tuning the full model significantly improves the model accuracy.

For instance, with the trigger magnitude set as 50, full-model tuning improves the ACC from 80.6% to 84.4%. Second, the fine-tuning strategy has a modest impact on the ASR of CTRL. For instance, with the trigger magnitude set as 50, the ASR under classifier-only and full-model tuning differs by only 2.2%. Finally, increasing the trigger magnitude generally improves the ASR under varying fine-tuning strategies. For instance, the ASR grows by 6.6% under full-model tuning if the trigger magnitude increases from 50 to 100.

Other factors. We have also explored the influence of other factors such as training epochs on CTRL. Due to the space limitations, the results are deferred to Appendix § B.

Q3: Ablation Study

Below we conduct an ablation study to understand the contribution of each component of CTRL to its effectiveness.

Trigger definition. Recall that CTRL defines the trigger patterns as specific perturbations to the spectral space of inputs. To evaluate the importance of this design, we consider an alternative trigger pattern, a randomly generated patch of input size. Specifically, we randomly generate an input-size patch and then project it to the same L_2 norm as the spectral trigger (*e.g.*, 0.7) for a proper comparison. Table 5 compares the performance of the spectral and random triggers. Observe that the spectral trigger significantly outperforms the random trigger in terms of ASR (*e.g.*, by around 75% on CIFAR-10 with SimCLR). We explore the underlying mechanisms of spectral triggers in § 5.1.

Trigger	Dataset	SimCLR		BYOL		SimSiam	
		ACC	ASR	ACC	ASR	ACC	ASR
Random	CIFAR-10	80.7%	10.7%	80.6%	10.7%	80.6%	10.3%
	CIFAR-100	48.2%	1.2%	51.1%	1.2%	52.3%	1.1%
Spectral	CIFAR-10	80.5%	85.3%	82.2%	61.9%	82.0%	74.9%
	CIFAR-100	47.6%	68.8%	50.8%	42.3%	52.6%	83.9%

Table 5. Performance of CTRL under varying trigger patterns.

Candidate selection. Besides randomly selecting candidate inputs to craft poisoning data in § 3.3, we consider alternative scenarios: *center* – we first train a clean encoder f on the reference data \bar{D} , compute the representation of each input in \bar{D} , and then select k candidates closest to the center in the feature space (measured by L_2 distance); and *core-set* – we cluster the class- t inputs in \bar{D} into k clusters in the feature space (*e.g.*, using k -means clustering) and select the inputs closest to the cluster centers as the candidates.

Table 6 compares their impact on the attack performance. We have the following observations. First, the random selector outperforms others on CIFAR-10. This may be explained by that over the relatively simple class distribution (*e.g.*, 10 classes), the random scheme is able to select a set of representative candidates of the underlying distribution. Second, no single selector dominates on CIFAR-100. This may be explained by that no single selector is able to fit the complex class distribution (*i.e.*, 100 classes) across all the

Dataset	Selector	SimCLR		BYOL		SimSiam	
		ACC	ASR	ACC	ASR	ACC	ASR
CIFAR-10	Random	80.5%	85.3%	82.2%	61.9%	82.0%	74.9%
	Center	81.2%	57.1%	80.0%	47.4%	80.8%	67.9%
	Core-set	80.3%	31.2%	81.7%	52.6%	81.7%	40.4%
CIFAR-100	Random	47.6%	68.8%	50.8%	42.3%	52.6%	83.9%
	Center	48.8%	78.1%	51.2%	54.7%	52.8%	78.6%
	Core-set	48.5%	54.6%	50.7%	64.7%	53.1%	53.9%

Table 6. Performance of CTRL with varying candidate selectors.

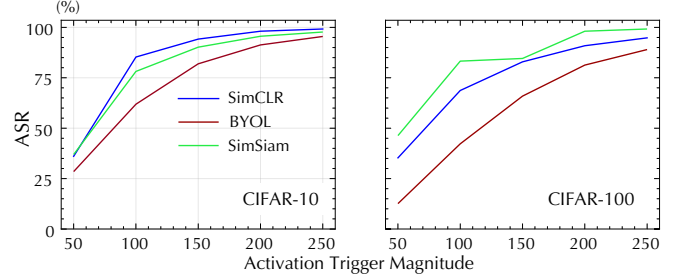


Figure 11: ASR of CTRL w.r.t the activation trigger magnitude on CIFAR-10 with SimCLR.

SSL methods. Thus, under the setting that the adversary is able to poison a limited amount of training data, the random selector is a practical choice.

Backdoor activation. Recall that CTRL allows the adversary to set triggers of different magnitude for crafting poisoning data (poisoning trigger) and activating backdoors (activation trigger) to optimize different metrics (*e.g.*, attack evasiveness versus effectiveness). We evaluate the influence of the activation trigger magnitude (with the poisoning trigger magnitude fixed as 50) on the attack performance at inference, with results summarized in Figure 11. As expected, increasing the activation trigger magnitude improves the attack effectiveness. For instance, on CIFAR-10 with SimCLR, as the activation trigger magnitude varies from 50 to 250, the ASR of CTRL increases from 36% to 99%. Note that as the activation trigger is only applied at inference, increasing the activation trigger magnitude does not affect the ACC.

5. Discussion

In this section, through the lens of CTRL, we compare the supervised and self-supervised trojan attacks and reveal the unique vulnerability incurred by the current design of SSL methods; further, we explore the fundamental challenges to defending against CTRL and self-supervised trojan attacks in general; finally, we discuss the limitations of this work. All the proofs are deferred to Appendix § A.

5.1. Comparison of Supervised and Self-supervised Trojan Attacks

While CTRL is simple, understanding how it works is non-trivial. Next, we study the mechanisms underlying CTRL both empirically and analytically.

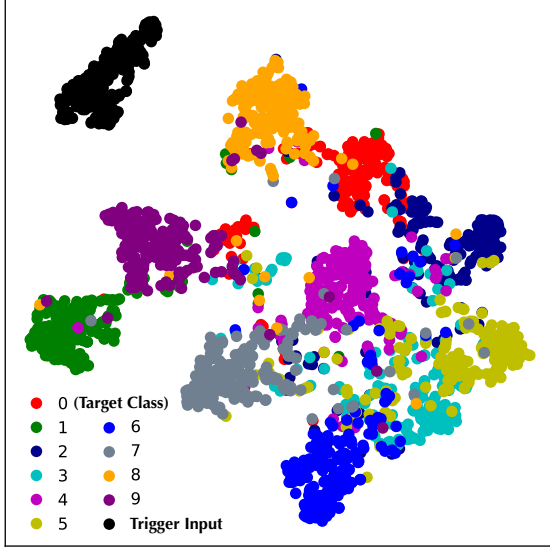


Figure 12: t -SNE visualization of the features of trigger-embedded and clean inputs in the supervised trojan attack (target-class input: red; trigger-embedded input: black).

To simplify the analysis, we assume the trigger embedding operator \oplus , which mixes clean input x with trigger r to produce trigger input x_* : $x_* = x \oplus r$, can be disentangled in the feature space. That is, $f(x_*) = (1 - \alpha)f(x) + \alpha f(r)$, where $\alpha \in (0, 1)$ denotes the mixing weight. This property applies to a range of linearly mixable encoders [55] such as over-parameterized linear model [24] and convolutional model [37].

Characterizing supervised trojan attacks. In supervised learning, the trojan attack associates the trigger r with the target label t via (implicitly) minimizing the objective defined in Eq (3). The success of this attack is often attributed to the model’s excess capacity [41], which “memorizes” both the function that classifies clean inputs and that misclassifies trigger inputs. Note that Eq (3) does not specify any constraints on the representations of trigger inputs. Thus, while associated with the same class, the trigger-embedded and target-class inputs are not necessarily proximate in the feature space.

To validate the analysis, we use CTRL to generate the poisoning data, pollute 1% of the training data across all the classes, and train the trojan model in a supervised setting for 20 epochs, which achieves 100% ASR and 83% ACC. We use t -SNE [49] to visualize the representations of trigger-embedded and clean inputs in the test set, with results shown in Figure 12. Although the clusters of trigger inputs (black) and target-class inputs (red) are assigned the same label, they are well separated in the feature space, indicating that supervised trojan attacks do not necessarily associate the trigger with the target class in the feature space. This finding also corroborates prior work [44].

Remark 1 – With the supervisory signal of labels, the supervised trojan attack directly associates the trigger pattern with the target-class label, while the trigger-embedded and target-class inputs are not necessarily aligned in the feature space.

Characterizing self-supervised trojan attacks. In SSL, as the label information is absent, it performs representation learning by optimizing the contrastive loss, which aligns the features of positive pairs (the augmented views of the same sample) while separating the features of negative pairs (the augmented views of different samples) if applicable. Next, through the lens of CTRL, we examine the effect of aligning the positive pairs of trigger inputs.

Consider trigger input $x_* = x \oplus r$, where x is a clean input from the adversary’s target class t , and its positive pair $x_*^+ = x^+ \oplus r^+$, where x^+ and r^+ are the augmented variants of x and r , respectively. With the output of f normalized to 1 and the cosine similarity as the similarity metric, by aligning the positive pair $(f(x_*), f(x_*^+))$, we have the following derivation:

$$f(x_*)^\top f(x_*^+) = \underbrace{(1 - \alpha)^2 f(x)^\top f(x^+)}_{\text{align clean inputs}} + \underbrace{\alpha^2 f(r)^\top f(r^+)}_{\text{align triggers}} + \underbrace{(1 - \alpha)\alpha(f(x)^\top z_r^+ + z_r^\top f(x^+))}_{\text{associate target class and trigger}} \quad (4)$$

Here, the first term aligns the positive pair (x, x^+) , which is functionally equivalent to aligning the corresponding clean inputs; the second term aligns the representations of trigger r and its augmented variant r^+ ; while the third term entangles the trigger with the clean input (from the target class) in the feature space. Next, we quantitatively characterize the amplitude of this entanglement effect. We first introduce the following two assumptions commonly observed in encoders trained using SSL [52].

Assumption 5.1. (Alignment) A well-trained encoder f tends to map a positive pair to similar features. Formally, for given input x , $f(x)^\top f(x^+) \geq (1 - \epsilon)$, where $\epsilon \in [0, 1)$ is a small non-negative number. In particular, by design, the trigger r is invariant to the augmentation operator: $f(r)^\top f(r^+) = 1$.

Assumption 5.2. (Uniformity) A well-trained encoder f tends to map inputs uniformly on the unit hyper-sphere \mathcal{S}^{d-1} of the feature space, preserving as much information of the data as possible. Thus, as the number of data points is large, the average angle θ between the features of a negative pair follows the distribution density function [1]:

$$h(\theta) = \frac{1}{\sqrt{\pi}} \frac{\Gamma(\frac{d}{2})}{\Gamma(\frac{d-1}{2})} (\sin \theta)^{d-2}, \quad \theta \in [0, \pi] \quad (5)$$

As the dimension d is high, most of the angles heavily concentrate around $\pi/2$.

Based on Assumption 5.1 and 5.2, consider a clean input \tilde{x} from a non-target class (with its trigger-embedded variant \tilde{x}_*), we can bound the entanglement effect between \tilde{x}_* with the target class as follows.

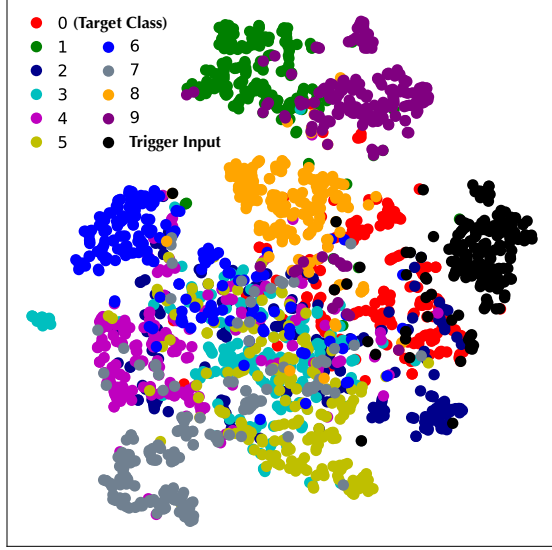


Figure 13: t -SNE visualization of the features of trigger-embedded and clean inputs in the self-supervised trojan attack (target-class input: red; trigger-embedded input: black).

Theorem 5.3. Let \tilde{x} be a clean input randomly sampled from a non-target class and x be a clean input randomly sampled from the target class t . The entanglement between the trigger-embedded input $\tilde{x}_* = \tilde{x} \oplus r$ and x in the feature space is lower bounded by: $\mathbb{E}[f(\tilde{x}_*)^\top f(x)] \geq \alpha - \frac{\epsilon}{2(1-\alpha)}$.

To validate the analysis above, we perform CTRL against SimCLR on CIFAR-10 and use t -SNE to visualize the features of trigger-embedded inputs and clean inputs in the test set, with results shown in Figure 13. Observed that in comparison with the supervised trojan attack (cf. Figure 12), the cluster of trigger-embedded inputs (black) and the cluster of target-class clean inputs (red) are highly entangled in the feature space, indicating that the self-supervised trojan attack takes effect by aligning the representations of trigger-embedded inputs and the target class.

Remark 2 – Without the supervisory signal of data labels, the self-supervised trojan attack takes effect by entangling trigger-embedded and target-class inputs in the feature space.

A deeper look at the entanglement effect. Besides revealing the attack mechanism underlying CTRL, Theorem 5.3 also sheds light on how to control the entanglement effect between trigger-embedded and target-class inputs by properly setting the trigger’s mixing weight α , which in turn influences the attack effectiveness. Intuitively, the entanglement is not a monotonic function of α : with overly small α , the influence of the trigger pattern on the entanglement is insignificant; with overly large α , the trigger pattern dominates the features of trigger-embedded inputs, which also negatively impacts the entanglement effect.

To validate our analysis, we empirically measure the entanglement effect between trigger-embedded and target-class inputs by varying the trigger magnitude in CTRL (cf. § 3.3). Specifically, we define *Entanglement Ratio* (ER), a

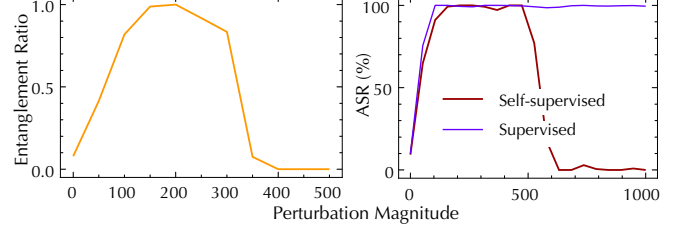


Figure 14: Entanglement effect and ASR w.r.t. the trigger magnitude.

metric to measure the entanglement effect, which extends the confusion ratio metric used in [53] to our setting. We sample $n = 800$ clean inputs from each class of CIFAR-10 to form the dataset \mathcal{D} ; we apply a set of $m = 10$ augmentation operators \mathcal{A} (sampled from the same distribution used by SSL) to each input $x \in \mathcal{D}$, which generates an augmented set $\mathcal{D}^+ = \{a(x)\}_{x \in \mathcal{D}, a \in \mathcal{A}}$. Further, we randomly sample 1,000 clean inputs disjoint with \mathcal{D} across all the classes and generate their trigger-embedded variants \mathcal{D}_* . For each $x_* \in \mathcal{D}_*$, we find its $K = 100$ nearest neighbors $\mathcal{N}_K(f(x_*))$ among \mathcal{D}^+ in the feature space and then measure the proportion of neighbors from the target class t :

$$\text{ER}(f) = \frac{1}{K} \mathbb{E}_{x_* \in \mathcal{D}_*} \mathbb{1}_{f(x_*) \in \mathcal{N}_K(f(x_*)), c(x_*)=t} \quad (6)$$

where t is the target class, $\mathbb{1}_p$ is an indicator function that returns 1 if p is true and 0 otherwise, $c(x^+)$ returns x^+ ’s label. Note that we use the label information here only for understanding the entanglement effect.

Intuitively, a larger ER indicates a stronger entanglement effect between the trigger-embedded inputs and the target class. We measure ER under varying trigger magnitude, with results shown in Figure 14. With the increase of trigger magnitude (a proxy of α), the entanglement effect first grows from 0 to 100% and then drops gradually to 0, which is consistent with our theoretical analysis. This observation implies that it is critical to optimally tune the entanglement effect to maximize the attack effectiveness.

To illustrate the correlation between entanglement effect and attack performance, Figure 14 also measures the ASR of CTRL under varying trigger magnitude (the same magnitude for the poisoning and activation triggers). Observe that ASR demonstrates a trend highly similar to ER with respect to trigger magnitude: it first increases to 100% and then drops to 0. Also notice that the trend of ASR lags behind ER. This may be explained as follows: the classifier divides the feature space into different classes; only when trigger-embedded and target-class inputs are separated sufficiently apart, the ASR starts to drop. In comparison, the ASR of supervised trojan attack increases to around 100% and maintains at that level, indicating its irrelevance to the entanglement effect.

Remark 3 – The entanglement effect between trigger-embedded and target-class inputs is a non-monotonic function of the trigger magnitude.

Adversarial robustness and trojan attacks. Prior work shows that SSL may benefit the robustness to adversarial

attacks [17]. However, our empirical evaluation and theoretical analysis suggest that this robustness benefit may not generalize to trojan attacks. We speculate that the representation-invariant property of SSL, which benefits adversarial robustness, may also be the very reason making SSL vulnerable to trojan attacks.

Intuitively, representation invariance indicates that different augmented views of the same input should share similar representations. Essentially, data augmentation and contrastive loss, two key ingredients of SSL, are designed to ensure this property [4], [11], [6]. Meanwhile, adversarial robustness indicates that adversarially augmented versions of the same input should share the same label (*i.e.*, label invariance). Thus, these two properties are aligned in principle; enforcing the invariance of intermediate representations tends to improve the variance of classification labels.

On the other hand, as shown in Figure 13, due to the overlap between the augmented views of trigger-embedded and target-class inputs, enforcing the representation invariance causes the trigger-embedded and target-class inputs to generate similar representations and essentially entangles them in the feature space, leading to the risk of trojan attacks. Therefore, the robustness of SSL to adversarial attacks may be at odds with its robustness to trojan attacks.

Remark 4 – The benefit of SSL for adversarial robustness may not generalize to trojan attacks.

5.2. Potential Defenses

Next, we explore the fundamental challenges to defending against CTRL and self-supervised trojan attacks in general.

Challenge 1: Label absence. Missing data labels not only challenges the adversary but also hinders the defender. For instance, many defenses against supervised trojan attacks attempt to filter poisoning inputs from training data, which typically require modeling the characteristics of each class [3], [51]. Due to label absence, such defenses are inapplicable to SSL. Relatedly, the defenses that rely on loss or gradient information are often ineffective against self-supervised trojan attacks. As an example,

Anti-backdoor learning (ABL) [29] is an input filtering defense that isolates trigger inputs and unlearns trojan models. Intuitively, the backdoor task is a much easier task compared to the original task; therefore, the loss of trigger inputs drops abruptly in early training epochs while the loss of clean inputs decreases at a steady pace. Leveraging this insight, ABL detects trigger inputs by measuring their loss and unlearns trojan models by conducting gradient descent on clean inputs and gradient ascent on detected trigger inputs.

Despite its effectiveness against supervised trojan attacks, it is challenging to extend ABL to self-supervised counterparts due to the following reason. In supervised attacks, the backdoor and original tasks are learned independently with respect to constant, ground-truth labels; ABL is able to segregate trigger inputs from clean inputs based on their loss

drop. In contrast, in self-supervised attacks, the backdoor and clean tasks are learned simultaneously with respect to constantly changing representations; aligning the positive pairs of trigger inputs also entangles trigger-embedded and target-class inputs. It is thus difficult to use loss drop as an effective indicator.

Challenge 2: Entanglement effect. Besides label absence, the entanglement between the representations of trigger and clean inputs also causes challenges for defenses that rely on the separability of trigger inputs.

Activation clustering (AC) [3] is another input inspection method. It trains the model using the training data that potentially contains poisoning inputs and collects the penultimate-layer activation of each input. Based on the assumption that in the target class, poisoning inputs form their own cluster that is small or far from the class center, AC detects the target class using the silhouette score of each class, with a higher score indicating that two clusters fit the data distribution better. Further, assuming that the adversary cannot poison more than half of the data, it considers the smaller cluster as the poisoning data. Due to the requirement for labeling, AC is inapplicable to SSL directly. Here, we assume the data labels are available and explore its effectiveness against CTRL on CIFAR-10 with SimCLR.

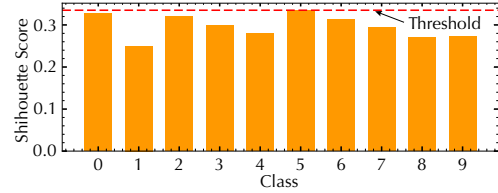


Figure 15: Evaluation results of activation clustering against CTRL.

From Figure 15, observe that AC fails to identify the target class (class 0), which has a lower score compared to other classes (*e.g.*, class 5), not to mention detecting the poisoning inputs. This may be attributed to the tight entanglement between the representations of poisoning and clean inputs.

STRIP [10] is a run-time input inspection method. Specifically, it assumes that the predictions of trigger inputs are invariant to perturbation due to the existence of trigger patterns, whereas the predictions of clean inputs may vary greatly with perturbation. For an incoming input, STRIP intentionally perturbs it (*e.g.*, superimposing various image patterns) and utilizes the randomness of predicted classes to detect trigger inputs. Since it is a run-time detection method, we use a well-trained full model (trojan encoder plus downstream classifier) to evaluate the effectiveness of STRIP. Following [10], we use false positive rate (FPR) and true positive rate (TPR) as the evaluation metrics, where FPR denotes the probability that a benign input is falsely detected as a trigger input, while TPR denotes the probability that a trigger input is correctly detected. A lower FPR and a higher TPR indicate more accurate detection.

Table 7 reports the effectiveness of STRIP against CTRL.

FPR	Decision Boundary	TPR
0.5%	0.56	0.5%
1.0%	0.65	1.1%
2.0%	0.75	2.0%

Table 7. Evaluation results of STRIP against CTRL.

Observe that STRIP is ineffective to detect trigger inputs generated by CTRL. For instance, with FRR fixed as 1.0%, the TPR of STRIP is as low as 1.1%, indicating that STRIP fails to distinguish trigger inputs from clean ones. This may also be explained by the entanglement effect: as the trigger and clean inputs share similar representations, the perturbation to them leads to similar measures.

Statistical Contamination Analyzer (SCAN) [44] detects trigger inputs based on the statistical properties of their representations. Specifically, it applies an EM algorithm to decompose an input into two terms: identity and variance; it then analyzes the representations in each class and identifies the target class most likely to be characterized by a mixture model. To explore the effectiveness of SCAN against CTRL, following [44], we first randomly sample 1,000 inputs from the testing set to build the decomposition model; we then use it to analyze a poisoning set with 5,000 trigger inputs and 5,000 clean inputs. We also use FPR and TPR to evaluate SCAN. Additionally, to compare the performance of SCAN against supervised and self-supervised trojan attacks, we also evaluate SCAN on two supervised trojan attacks: one with the same spectral trigger as CTRL and the other with a random 5×5 image patch as the trigger.

FPR	TPR		
	CTRL	Supervised (spectral)	Supervised (patch)
0.5%	28.0%	63.0%	97.0%
1.0%	28.0%	66.5%	97.0%
2.0%	28.0%	68.0%	97.0%

Table 8. Evaluation results of SCAN against CTRL.

Table 8 summarizes the results. We have the following observations. First, it is more challenging for SCAN to detect spectral triggers than patch triggers. For instance, with FPR fixed as 0.5%, the TPR of SCAN differs by over 34% on the spectral and patch triggers. The difference may be explained by that compared with patch triggers, spectral triggers are more evasive by design (details in § 3), which can hardly be characterized by a mixture model. Even if the target class is correctly identified, many trigger inputs may still fall into the cluster of clean inputs. Moreover, between supervised and self-supervised trojan attacks, SCAN is less effective against self-supervised attacks. For instance, with the same spectral trigger, SCAN detects over 63.0% of trigger inputs under the supervised attack, while it only detects 28.0% under CTRL. This may be explained by the entanglement between the representations of the trigger and clean inputs, while SCAN relies on the separability of trigger inputs in the feature space.

Challenge 3: Accuracy-robustness trade-off. Defending against self-supervised trojan attacks also faces the dilemma of trading model accuracy for attack robustness.

Augmentation ablation selectively applies some augmentations while suppressing the others, which is an intuitive defense against self-supervised trojan attacks [30]. As one critical ingredient of SSL, augmentation operators dictate how intra-class inputs are aligned and how inter-class inputs are separated [53]. To explore their influence on the performance of CTRL, we ablate each operator from the operator set and evaluate the corresponding ACC and ASR of CTRL on CIFAR-10, with results summarized in Table 9.

Augmentation	SimCLR		BYOL		SimSiam	
	ACC	ASR	ACC	ASR	ACC	ASR
w/o <i>RandomResizeCrop</i>	55.9%	11.6%	34.9%	16.3%	10.3%	25.9%
w/o <i>RandomHorizontalFlip</i>	81.3%	53.4%	81.8%	47.3%	80.6%	50.7%
w/o <i>ColorJitter</i>	74.6%	18.3%	77.2%	10.4%	74.4%	11.9%
w/o <i>RandomGrayscale</i>	74.6%	99.8%	75.4%	26.6%	74.9%	12.2%

Table 9. Impact of augmentation operators on CTRL.

It is observed that different operators have varying impacts. In particular, compared to other operators, *RandomResizeCrop* and *ColorJitter* have more influence on both the model’s accuracy and CTRL’s effectiveness. For instance, without *RandomResizeCrop*, the ACC and ASR of the victim model trained by SimCLR drops by 34.6% and 73.7%, respectively (*cf.* Table 2). This may be explained by that as two strong augmentations [53], *RandomResizeCrop* and *ColorJitter* generate highly varying augmented views, thereby impacting how intra-class inputs are aligned and also trigger-embedded and target-class inputs are entangled. This also indicates that removing specific augmentations may not be a viable defense against CTRL, due to its negative impact on the model accuracy.

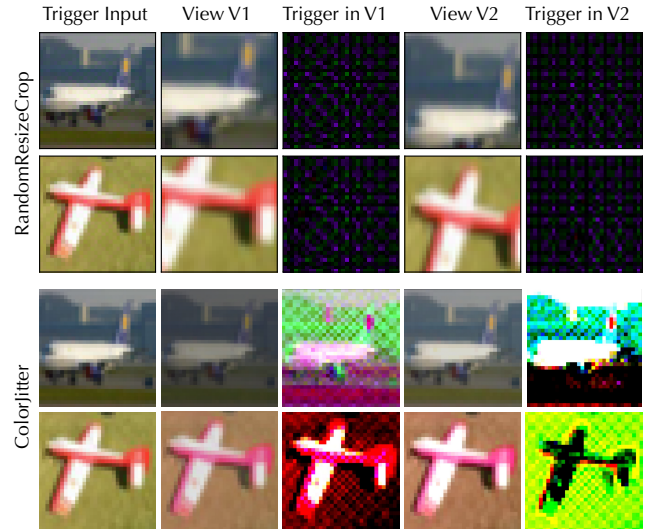


Figure 16: Visualization of augmented views under strong augmentations (the triggers are magnified by 20 times to be evident).

To provide an intuitive understanding of the influence of augmentation operators on spectral triggers, we visualize the augmented views of sample inputs under *RandomResizeCrop* and *ColorJitter* in Figure 16. Observe that the triggers are preserved even under strong augmentations, which realizes symmetric augmented views, leading to high utilization of

poisoning data.

5.3. Limitations and Future Work

Next, we discuss the limitations of this work.

Optimal trigger design. In CTRL, we define the trigger pattern based on our empirical heuristics, which is not necessarily optimal in terms of attack effectiveness. We attempt several solutions to optimize the trigger design, including (i) alternating between optimizing the trigger and training the model and (ii) optimizing the trigger with respect to a pre-trained model. However, we find that such optimized triggers fail to improve the attack effectiveness while the ASR even declines to 0 in the later training phase. We speculate that this is because the trigger optimization may follow a “shortcut” to decrease the contrastive loss. More concretely, the pre-trained encoder may focus more on the trigger features of trigger-embedded inputs in Eq (8), while failing to entangle trigger-embedded and target-class inputs in the feature space. We consider how to rigorously optimize the trigger design in CTRL as our ongoing research.

Optimal poisoning strategy. To be practical, we assume the adversary has no knowledge or control over which inputs are selected by the victim in training. We also consider different strategies in which random or representative inputs are poisoned and find that none of the strategies dominates across all the models and SSL methods. It is interesting to explore the optimal poisoning strategy if certain prior knowledge about the victim’s training data is available.

Other malicious attacks. Above, we mainly investigate the vulnerability of SSL to trojan attacks, while SSL is also the target for other types of malicious attacks (*e.g.*, membership inference [31], [15]). We consider understanding the inherent connections between different attacks within the context of SSL as one promising direction for future research.

Other SSL domains. In this work, we mainly focus on image classification tasks, while SSL has been applied in many other domains such as natural language processing and graph learning. We consider extending CTRL to such domains as our future work. Besides, based on our empirical and analytical studies, developing effective defenses in these domains represents non-trivial challenges.

6. Related work

In addition to the aforementioned related work, we further survey the literature most relevant to this work.

Self-supervised learning. Recent years have witnessed the striding advances of self-supervised learning (SSL) [4], [11], [6]. Meanwhile, the popularity of SSL also spurs intensive research on its security properties. Existing work has explored the adversarial robustness of SSL [23], [9]. It is shown that, as a nice side effect, obviating the reliance on data labeling

may benefit the robustness to adversarial examples, label corruption, and common input corruptions [17]. Yet, whether this robustness benefit also generalizes to other types of attacks remains an open question. This work explores this question in the context of trojan attacks.

Trojan attacks. As one major threat to machine learning security, trojan attacks inject malicious backdoors into the victim’s model during training and activate such backdoors at inference. Many trojan attacks have been proposed for the supervised learning setting, which can be categorized along (i) attack targets – input-specific [42], class-specific [44], or any-input [12], (ii) attack vectors – polluting training data [33] or releasing trojan models [21], and (iii) optimization metrics – attack effectiveness [35], transferability [54], or attack evasiveness [7], [42], [47], [56].

Trojan attacks are of particular interest for SSL: as SSL-trained models are subsequently used in various downstream tasks, trojan attacks may cause widespread damage. Yet, most supervised trojan attacks are inapplicable to SSL due to the absence of labeling. Recent work has explored new ways of injecting backdoors into SSL-trained models [22], [39], [30], [2]. Most related to this work, BadEncoder [22] injects backdoors into pre-trained encoders and releases trojan models to victims in downstream tasks; SSLBackdoor [39] generates poisoning data using a specific image patch as the trigger pattern; PoisonedEncoder [30] poisons the training data by randomly combining target inputs with reference inputs. However, all these attacks seem to under-perform their supervised counterparts, raising the intriguing question: is SSL inherently more robust than supervised learning to trojan attacks? This work gives a negative answer to this question and reveals that the current design of SSL methods entails unique vulnerability to trojan attacks.

Trojan defenses. To mitigate the threats of trojan attacks, many defenses have been proposed, which can be categorized according to their strategies [36]: (i) input filtering, which purges poisoning examples from training data [45], [3]; (ii) model inspection, which determines whether a given model is trojaned and, if so, recovers the target class and the potential trigger [25], [18], [32], [50]; and (iii) input inspection, which detects trigger inputs at inference time [44], [10], [43].

However, designed for supervised trojan attacks, the effectiveness of these defenses in the SSL setting remains under-explored. This work systematically evaluates these defenses against CTRL and identifies the fundamental challenges to defending against self-supervised trojan attacks.

7. Conclusion

This work conducts a systematic study on the vulnerability of self-supervised learning (SSL) to trojan attacks. By developing and evaluating CTRL, a simple yet effective self-supervised trojan attack, we demonstrate that SSL is highly susceptible to trojan attacks. Further, both empirically and analytically, we reveal that the representation invariance property of SSL, which benefits adversarial robustness, may

also account for the vulnerability of SSL to trojan attacks. Finally, we discuss potential countermeasures and identify the unique challenges to defending against self-supervised trojan attacks. We hope our findings will shed light on developing more robust SSL methods.

References

- [1] Tony Cai, Jianqing Fan, and Tiejing Jiang. Distributions of angles in random packing on spheres. *Journal of Machine Learning Research*, 14(21):1837–1864, 2013.
- [2] Nicholas Carlini and Andreas Terzis. Poisoning and backdooring contrastive learning. In *Proceedings of International Conference on Learning Representations (ICLR)*, 2022.
- [3] Bryant Chen, Wilka Carvalho, Nathalie Baracaldo, Heiko Ludwig, Benjamin Edwards, Taesung Lee, Ian Molloy, and Biplav Srivastava. Detecting backdoor attacks on deep neural networks by activation clustering. *ArXiv e-prints*, 2018.
- [4] Ting Chen, Simon Kornblith, Mohammad Norouzi, and Geoffrey Hinton. A simple framework for contrastive learning of visual representations. In *Proceedings of IEEE Conference on Machine Learning (ICML)*, 2020.
- [5] Xinlei Chen, Haoqi Fan, Ross Girshick, and Kaiming He. Improved baselines with momentum contrastive learning. *ArXiv e-prints*, 2020.
- [6] Xinlei Chen and Kaiming He. Exploring simple siamese representation learning. In *Proceedings of IEEE Conference on Computer Vision and Pattern Recognition (CVPR)*, 2021.
- [7] Xinyun Chen, Chang Liu, Bo Li, Kimberly Lu, and Dawn Song. Targeted backdoor attacks on deep learning systems using data poisoning. *ArXiv e-prints*, 2017.
- [8] J. Deng, W. Dong, R. Socher, L. Li, Kai Li, and Li Fei-Fei. ImageNet: A Large-scale Hierarchical Image Database. In *Proceedings of IEEE Conference on Computer Vision and Pattern Recognition (CVPR)*, 2009.
- [9] Lijie Fan, Sijia Liu, Pin-Yu Chen, Gaoyuan Zhang, and Chuang Gan. When does contrastive learning preserve adversarial robustness from pretraining to finetuning? In *Proceedings of Advances in Neural Information Processing Systems (NeurIPS)*, 2021.
- [10] Yansong Gao, Change Xu, Derui Wang, Shiping Chen, Damith C Ranasinghe, and Surya Nepal. Strip: A defence against trojan attacks on deep neural networks. In *Proceedings of Annual Computer Security Applications Conference (ACSAC)*, 2019.
- [11] Jean-Bastien Grill, Florian Strub, Florent Altché, Corentin Tallec, Pierre Richemond, Elena Buchatskaya, Carl Doersch, Bernardo Avila Pires, Zhaohan Guo, Mohammad Gheshlaghi Azar, et al. Bootstrap your own latent - a new approach to self-supervised learning. In *Proceedings of Advances in Neural Information Processing Systems (NeurIPS)*, 2020.
- [12] Tianyu Gu, Brendan Dolan-Gavitt, and Siddharth Garg. Badnets: Identifying vulnerabilities in the machine learning model supply chain. *ArXiv e-prints*, 2017.
- [13] Kaiming He, Haoqi Fan, Yuxin Wu, Saining Xie, and Ross Girshick. Momentum contrast for unsupervised visual representation learning. In *Proceedings of IEEE Conference on Computer Vision and Pattern Recognition (CVPR)*, 2020.
- [14] Kaiming He, Xiangyu Zhang, Shaoqing Ren, and Jian Sun. Deep Residual Learning for Image Recognition. In *Proceedings of IEEE Conference on Computer Vision and Pattern Recognition (CVPR)*, 2016.
- [15] Xinlei He and Yang Zhang. Quantifying and mitigating privacy risks of contrastive learning. In *Proceedings of ACM SAC Conference on Computer and Communications (CCS)*, 2021.
- [16] S Hemalatha, U Dinesh Acharya, and A Renuka. Comparison of secure and high capacity color image steganography techniques in rgb and ycbcr domains. *ArXiv e-prints*, 2013.
- [17] Dan Hendrycks, Mantas Mazeika, Saurav Kadavath, and Dawn Song. Using self-supervised learning can improve model robustness and uncertainty. In *Proceedings of Advances in Neural Information Processing Systems (NeurIPS)*, 2019.

- [18] Xijie Huang, Moustafa Alzantot, and Mani Srivastava. Neuroninspect: Detecting backdoors in neural networks via output explanations. *ArXiv e-prints*, 2019.
- [19] Forrest N Iandola, Song Han, Matthew W Moskewicz, Khalid Ashraf, William J Dally, and Kurt Keutzer. Squeezenet: Alexnet-level accuracy with 50x fewer parameters and < 0.5 mb model size. *ArXiv e-prints*, 2016.
- [20] Ashish Jaiswal, Ashwin Ramesh Babu, Mohammad Zaki Zadeh, Debapriya Banerjee, and Fillia Makedon. A survey on contrastive self-supervised learning. *Technologies*, 9(1):2, 2020.
- [21] Yujie Ji, Xinyang Zhang, Shouling Ji, Xiapu Luo, and Ting Wang. Model-Reuse Attacks on Deep Learning Systems. In *Proceedings of ACM SAC Conference on Computer and Communications (CCS)*, 2018.
- [22] Jinyuan Jia, Yupei Liu, and Neil Zhenqiang Gong. Badencoder: Backdoor attacks to pre-trained encoders in self-supervised learning. In *Proceedings of IEEE Symposium on Security and Privacy (S&P)*, 2021.
- [23] Ziyu Jiang, Tianlong Chen, Ting Chen, and Zhangyang Wang. Robust pre-training by adversarial contrastive learning. In *Proceedings of Advances in Neural Information Processing Systems (NeurIPS)*, 2020.
- [24] Li Jing, Pascal Vincent, Yann LeCun, and Yuandong Tian. Understanding dimensional collapse in contrastive self-supervised learning. In *Proceedings of International Conference on Learning Representations (ICLR)*, 2022.
- [25] Soheil Kolouri, Aniruddha Saha, Hamed Pirsiavash, and Heiko Hoffmann. Universal litmus patterns: Revealing backdoor attacks in cnns. In *Proceedings of IEEE Conference on Computer Vision and Pattern Recognition (CVPR)*, 2020.
- [26] Alex Krizhevsky and Geoffrey Hinton. Learning Multiple Layers of Features from Tiny Images. *Technical report, University of Toronto*, 2009.
- [27] Alex Krizhevsky, Vinod Nair, and Geoffrey Hinton. Cifar-100 (canadian institute for advanced research).
- [28] Shaofeng Li, Benjamin Zi Hao Zhao, Jiahao Yu, Minhui Xue, Dali Kaafar, and Haojin Zhu. Invisible backdoor attacks against deep neural networks. *ArXiv e-prints*, 2019.
- [29] Yige Li, Xixiang Lyu, Nodens Koren, Lingjuan Lyu, Bo Li, and Xingjun Ma. Anti-backdoor learning: Training clean models on poisoned data. In *Proceedings of Advances in Neural Information Processing Systems (NeurIPS)*, 2021.
- [30] Hongbin Liu, Jinyuan Jia, and Neil Zhenqiang Gong. Poisonedencoder: Poisoning the unlabeled pre-training data in contrastive learning. In *Proceedings of USENIX Security Symposium (SEC)*, 2022.
- [31] Hongbin Liu, Jinyuan Jia, Wenjie Qu, and Neil Zhenqiang Gong. Encodermi: Membership inference against pre-trained encoders in contrastive learning. In *Proceedings of ACM SAC Conference on Computer and Communications (CCS)*, 2021.
- [32] Yingqi Liu, Wen-Chuan Lee, Guan hong Tao, Shiqing Ma, Yousra Aafer, and Xiangyu Zhang. Abs: Scanning neural networks for back-doors by artificial brain stimulation. In *Proceedings of ACM Conference on Computer and Communications (CCS)*, 2019.
- [33] Yingqi Liu, Shiqing Ma, Yousra Aafer, Wen-Chuan Lee, Juan Zhai, Weihang Wang, and Xiangyu Zhang. Trojaning attack on neural networks. In *Proceedings of Network and Distributed System Security Symposium (NDSS)*, 2018.
- [34] Ningning Ma, Xiangyu Zhang, Hai-Tao Zheng, and Jian Sun. Shufflenet v2: Practical guidelines for efficient cnn architecture design. In *Proceedings of European Conference on Computer Vision (ECCV)*, 2018.
- [35] Ren Pang, Hua Shen, Xinyang Zhang, Shouling Ji, Yevgeniy Vorobeychik, Xiapu Luo, Alex Liu, and Ting Wang. A tale of evil twins: Adversarial inputs versus poisoned models. In *Proceedings of ACM Conference on Computer and Communications (CCS)*, 2020.
- [36] Ren Pang, Zheng Zhang, Xiangshan Gao, Zhaohan Xi, Shouling Ji, Peng Cheng, and Ting Wang. Trojanzoo: Towards unified, holistic, and practical evaluation of neural backdoors. In *Proceedings of IEEE European Symposium on Security and Privacy (Euro S&P)*, 2020.
- [37] Philipp Petersen and Felix Voigtlaender. Equivalence of approximation by convolutional neural networks and fully-connected networks. *Proceedings of the American Mathematical Society*, 148(4):1567–1581, 2020.
- [38] Md Rahman et al. A dwt, dct and svd based watermarking technique to protect the image piracy. *ArXiv e-prints*, 2013.
- [39] Aniruddha Saha, Ajinkya Tejankar, Soroush Abbasi Koohpayegani, and Hamed Pirsiavash. Backdoor attacks on self-supervised learning. *ArXiv e-prints*, 2021.
- [40] Mark Sandler, Andrew Howard, Menglong Zhu, Andrey Zhmoginov, and Liang-Chieh Chen. Mobilenetv2: Inverted residuals and linear bottlenecks. In *Proceedings of IEEE Conference on Computer Vision and Pattern Recognition (CVPR)*, 2018.
- [41] Naren Sarayu Manoj and Avrim Blum. Excess capacity and backdoor poisoning. In *Proceedings of Advances in Neural Information Processing Systems (NeurIPS)*, 2021.
- [42] Ali Shafahi, W. Ronny Huang, Mahyar Najibi, Octavian Suciu, Christoph Studer, Tudor Dumitras, and Tom Goldstein. Poison frogs! targeted clean-label poisoning attacks on neural networks. In *Proceedings of Advances in Neural Information Processing Systems (NeurIPS)*, 2018.
- [43] Mahesh Subedar, Nilesh Ahuja, Ranganath Krishnan, Ibrahimia J Ndiour, and Omesh Tickoo. Deep probabilistic models to detect data poisoning attacks. *ArXiv e-prints*, 2019.
- [44] Di Tang, XiaoFeng Wang, Haixu Tang, and Kehuan Zhang. Demon in the variant: Statistical analysis of dnns for robust backdoor contamination detection. In *Proceedings of USENIX Security Symposium (SEC)*, 2020.
- [45] Brandon Tran, Jerry Li, and Aleksander Madry. Spectral signatures in backdoor attacks. In *Proceedings of Advances in Neural Information Processing Systems (NeurIPS)*, 2018.
- [46] Dimitris Tsipras, Shibani Santurkar, Logan Engstrom, Alexander Turner, and Aleksander Madry. Robustness may be at odds with accuracy. In *Proceedings of International Conference on Learning Representations (ICLR)*, 2019.
- [47] Alexander Turner, Dimitris Tsipras, and Aleksander Madry. Label-consistent backdoor attacks. *ArXiv e-prints*, 2019.
- [48] Aaron van den Oord, Yazhe Li, and Oriol Vinyals. Representation learning with contrastive predictive coding. *ArXiv e-prints*, 2018.
- [49] Laurens Van der Maaten and Geoffrey Hinton. Visualizing data using t-sne. *Journal of Machine Learning Research*, 9(11), 2008.
- [50] B. Wang, Y. Yao, S. Shan, H. Li, B. Viswanath, H. Zheng, and B. Y. Zhao. Neural cleanse: Identifying and mitigating backdoor attacks in neural networks. In *Proceedings of IEEE Symposium on Security and Privacy (S&P)*, 2019.
- [51] Tong Wang, Yuan Yao, Feng Xu, Shengwei An, Hanghang Tong, and Ting Wang. An invisible black-box backdoor attack through frequency domain. In *Proceedings of European Conference on Computer Vision (ECCV)*, 2022.
- [52] Tongzhou Wang and Phillip Isola. Understanding contrastive representation learning through alignment and uniformity on the hypersphere. In *Proceedings of IEEE Conference on Machine Learning (ICML)*, 2020.
- [53] Yifei Wang, Qi Zhang, Yisen Wang, Jiansheng Yang, and Zhouchen Lin. Chaos is a ladder: A new theoretical understanding of contrastive learning via augmentation overlap. *ArXiv e-prints*, 2022.
- [54] Yuanshun Yao, Huiying Li, Haitao Zheng, and Ben Y. Zhao. Latent backdoor attacks on deep neural networks. In *Proceedings of ACM Conference on Computer and Communications (CCS)*, 2019.

- [55] Hongyi Zhang, Moustapha Cisse, Yann N. Dauphin, and David Lopez-Paz. mixup: Beyond empirical risk minimization. In *Proceedings of International Conference on Learning Representations (ICLR)*, 2018.
- [56] Shihao Zhao, Xingjun Ma, Xiang Zheng, James Bailey, Jingjing Chen, and Yu-Gang Jiang. Clean-label backdoor attacks on video recognition models. In *Proceedings of IEEE Conference on Computer Vision and Pattern Recognition (CVPR)*, 2020.

Appendix A. Proofs

Theorem 5.3. According to Assumption 5.1, we have

$$f(x_*)^\top f(x_*^+) \geq (1 - \epsilon) \quad (7)$$

In other words,

$$(1 - \alpha)^2 f(x)^\top f(x^+) + \alpha^2 f(r)^\top f(r^+) + \alpha(1 - \alpha)(f(x)^\top f(r^+) + f(r)^\top f(x^+)) \geq (1 - \epsilon).$$

Since both $f(x)^\top f(x^+)$ and $f(r)^\top f(r^+)$ are no larger than 1, we have

$$\begin{aligned} & \alpha(1 - \alpha)(f(x)^\top f(r^+) + f(r)^\top f(x^+)) \\ & \geq (1 - \epsilon) - (1 - \alpha)^2 f(x)^\top f(x^+) - \alpha^2 f(r)^\top f(r^+) \\ & \geq (1 - \epsilon) - (1 - \alpha)^2 - \alpha^2 \\ & = 2\alpha(1 - \alpha) - \epsilon \end{aligned}$$

Then, based on Assumption 5.1, we have

$$f(x)^\top f(r) \geq 1 - \frac{\epsilon}{2\alpha(1 - \alpha)}. \quad (8)$$

For \tilde{x}_* and x , we have

$$f(\tilde{x}_*)^\top f(x) = (1 - \alpha)f(\tilde{x})^\top f(x) + \alpha f(r)^\top f(x)$$

Since \tilde{x} and x are a negative pair, based on Assumption 5.2, we have

$$\begin{aligned} \mathbb{E}[f(\tilde{x}_*)^\top f(x)] & \geq \alpha(1 - \frac{\epsilon}{2\alpha(1 - \alpha)}) \\ & \geq \alpha - \frac{\epsilon}{2(1 - \alpha)} \end{aligned} \quad (9)$$

For a well-trained f , ϵ is a constant. Thus, both Eq (8) and Eq (9) are functions that first increase and then decrease with respect to $\alpha \in (0, 1)$. \square

Appendix B. More Details of Experiments

B.1. Dataset

For each dataset, we split it as a training set and a testing set according to its default setting. Specifically, both CIFAR-10 and CIFAR-100 are split into 50,000 and 10,000 images for training and testing, respectively; ImageNet-100 is split as 130,000 training and 5,000 testing images; while GTSRB is split into 39,209 training and 12,630 testing images.

B.2. Data Augmentation

For convenience, we describe the details of data augmentations in a PyTorch style. Specifically, following prior work [6], [4], we use geometric augmentation operators including *RandomResizeCrop* (of scale [0.2, 1.0]) and *RandomHorizontalFlip*. Besides, we use *ColorJitter* with [brightness, contrast, saturation, hue] of strength [0.4, 0.4, 0.4, 0.1] with an application probability of 0.8 and *RandomGrayscale* with an application probability of 0.2.

B.3. Encoder Training

We use the training set of each dataset to conduct contrastive learning. We show the hyper-parameters setting for each contrastive learning algorithm in Table 10, which is fixed across all the datasets.

Hyper-parameter	SSL Method		
	SimCLR	BYOL	SimSiam
Optimizer	SGD	SGD	SGD
Learning Rate	0.5	0.06	0.06
Momentum	0.9	0.9	0.9
Weight Decay	1e-4	1e-4	5e-4
Epochs	500	500	500
Batch Size	512	512	512
Temperature	0.5	-	-
Moving Average	-	0.996	-

Table 10. Hyper-parameters of encoder training.

B.4. Classifier Training

Without explicit specification, we randomly sample 50 examples from each class of the corresponding testing set to train the downstream classifier. We show the hyper-parameters of classifier in Table 11.

Hyper-parameter	Setting
Optimizer	SGD
Batch Size	512
Learning Rate	0.2
Momentum	0.9
Scheduler	Cosine Annealing
Epochs	20

Table 11. Hyper-parameters of classifier training.

B.5. Evaluation

We evaluate ACC using the corresponding testing set. For ASR, we apply CTRL on the full testing set and measure the ratio that the trigger input is classified to the target class. All the experiments are performed on a workstation equipped with Intel(R) Xeon(R) Silver 4314 CPU @ 2.40GHz, 512GB RAM, and four NVIDIA A6000 GPUs.

B.6. More Results

Training Epochs. Typically, SSL benefits from more training epochs [4]. We evaluate the impact of training epochs on the

performance of CTRL. Figure 17 shows the ACC and ASR of CTRL as the number of epochs varies from 600 to 1,000.

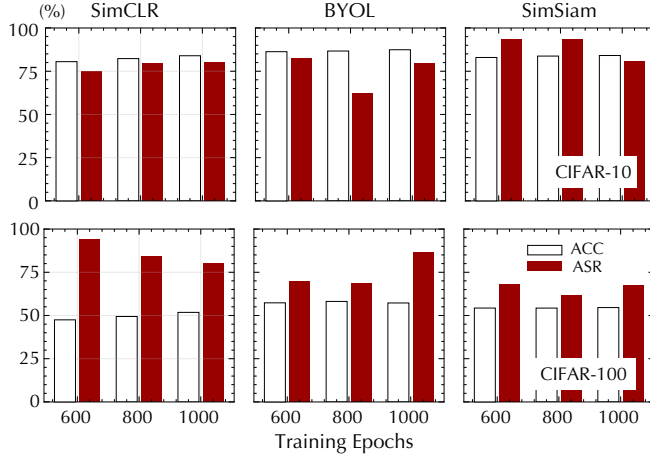


Figure 17: Performance of CTRL w.r.t. the number of epochs.

Observe that as the number of epochs increases, the ACC of CTRL gradually grows, while the ASR remains at a high level. For example, on CIFAR-10 with SimCLR, when the number of epochs increases from 600 to 1,000, the ACC also increases from 80.52% to 83.94%, and the ASR remains above 75%. In a few cases, the ASR slightly drops. We speculate this is caused by the random data augmentation process used in contrastive learning algorithms. Side evidence is that on CIFAR-10 with BYOL, the ASR first slightly decreases and then remains above 80%. In general, the number of training epochs has a limited impact on the effectiveness of CTRL.

Visualization. Here, we visualize the trojan model’s explanations (in the form of heat maps) when fed with clean and corresponding trigger inputs, which provides an intuitive understanding of the model’s behavior. Specifically, we randomly sample inputs that meet the requirements: (i) the clean inputs are classified correctly; (ii) the corresponding trigger inputs are misclassified to the target class. We use GradCam as the interpretation method.

Figure 18 shows the heat map of sample inputs. Observe that for given clean and trigger inputs, the trojan model focuses on fairly different regions of the images, indicating that the trigger pattern significantly shifts the representation of the clean input.

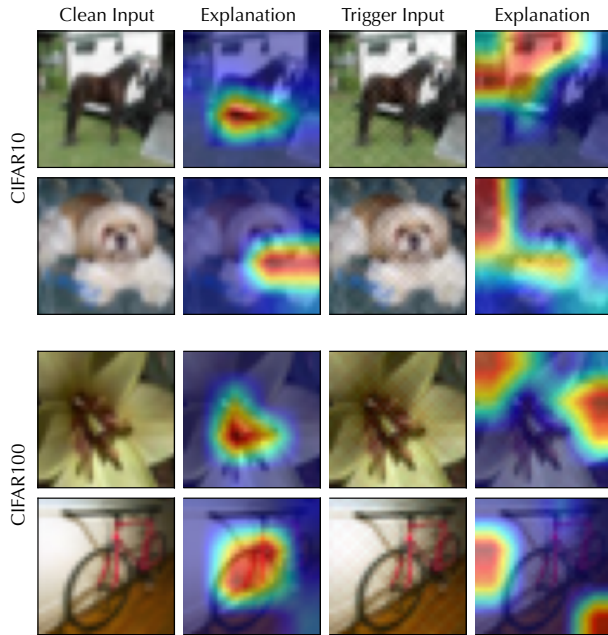


Figure 18: Explanations for sample clean and trigger inputs.